Enhanced sensitivity of oceanic CO_2 uptake to dust deposition by iron-light colimitation

Levin Nickelsen[1] and Andreas Oschlies[1]

Corresponding author: L. Nickelsen, GEOMAR Helmholtz Centre for Ocean Research Kiel, Duesternbrooker Weg 20, 24105 Kiel, Germany. (lnickelsen@geomar.de)

[1]GEOMAR, Helmholtz Centre for Ocean Research Kiel, Kiel, Germany.

This article has been accepted for publication and undergone full peer review but has not been through the copyediting, typesetting, pagination and proofreading process, which may lead to differences between this version and the Version of Record. Please cite this article as doi: 10.1002/2014GL062969

The iron hypothesis suggests that in large areas of the ocean phytoplankton growth and thus photosynthetic CO_2-uptake is limited by the micronutrient iron. Phytoplankton requires iron in particular for nitrate uptake, light harvesting and electron transport in photosynthesis, suggesting a tight coupling of iron and light limitation. One important source of iron to the open ocean is dust deposition. Previous global biogeochemical modeling studies have suggested a low sensitivity of oceanic CO_2-uptake to changes in dust deposition. Here we show that this sensitivity is increased significantly when iron-light colimitation, i.e. the impact of iron bioavailability on light harvesting capabilities, is explicitly considered. Accounting for iron-light colimitation increases the shift of export production from tropical and subtropical regions to the higher latitudes of subpolar regions at high dust deposition and amplifies iron limitation at low dust deposition. Our results re-emphasize the role of iron as a key limiting nutrient for phytoplankton.

1. Introduction

Low concentrations of the micronutrient iron limit primary production in vast areas of the ocean and in particular in most parts of the Southern Ocean [*Boyd and Ellwood*, 2010]. One of the major sources of iron to the ocean is dust deposition that is suggested to be coupled intimately to climate [*Martínez-Garcia et al.*, 2011]. While today dust deposition to the Southern Ocean is very low, the iron hypothesis [*Martin*, 1990] states that enhanced dust deposition to the Southern Ocean during the last glacial maximum triggered additional export of organically bound carbon and therefore decreased atmospheric CO_2 concentrations. Although a recent modeling study estimates only an increase of 2 ppmv in preindustrial atmospheric CO_2 when dust deposition is shut off completely [*Tagliabue et al.*, 2014], other studies suggest that decreasing dust deposition in the future such as predicted by *Mahowald et al.* [2006] may possibly lead to more severe iron limitation and a larger reduction in oceanic CO_2 uptake by phytoplankton [*Parekh et al.*, 2006; *Tagliabue et al.*, 2008]. The role of iron in regulating the oceanic CO_2 uptake is thus important for understanding past and possibly future atmospheric CO_2 levels.

From a biological point of view iron limitation in coupled biogeochemical ocean circulation models has, until now, been treated in a very simplistic way and interactions with other limiting nutrients and factors are often neglected. Observations show that iron limitation of phytoplankton growth is created by the requirement of iron for nitrate uptake, for proteins in the electron transport chain, for synthesizing chlorophyll and photoreaction centers and the functioning of light harvesting antennae [*Sunda and Huntsman*, 1997; *Behrenfeld and Milligan*, 2013]. Although physiological adaptation of polar phytoplank-

ton species to low iron concentrations may compensate for some of the positive effect of iron on light harvesting capabilities [*Strzepek et al.*, 2011, 2012], incubation experiments show elevated light harvesting capabilities of phytoplankton after adding iron [*Feng et al.*, 2010]. However, in most biogeochemical models that have been used to investigate the sensitivity of ocean biogeochemistry and CO_2 uptake to dust deposition, iron limitation is included as a further Monod term in a minimum function [*Bopp et al.*, 2003; *Moore and Braucher*, 2008; *Parekh et al.*, 2008; *Tagliabue et al.*, 2009a] while in explicit quota models such as in *Tagliabue et al.* [2009a, 2014] iron uptake is allowed to continue also under light limiting conditions. Only the recent model of *Galbraith et al.* [2010] explicitly describes the impact of iron limitation on the chlorophyll-to-carbon ratio and the initial slope of how irradiance is processed into photosynthesis as observed in culture and field experiments [*Greene et al.*, 1991; *Davey and Geider*, 2001; *Hopkinson et al.*, 2007; *Moore et al.*, 2007; *Hopkinson and Barbeau*, 2008]. The way the influence of iron limitation on light limitation is implemented in this model leads to parallel changes in the light-limited slope and light-saturated rate of photosynthesis with iron concentrations (Figure 1). The increase of the maximum growth rate only, as illustrated in Figure 1, is the response to additional iron as it is often treated in the other models. Here, in addition, also the initial slope increases. This response of both, maximum growth rate and initial slope, to the addition of iron is also observed in culture experiments [*Behrenfeld et al.*, 2004; *Behrenfeld and Milligan*, 2013].

The model used here has been shown to perform well in simulating the observed present-day global surface iron and phosphate concentrations while the agreement to observations

decreases if iron limitation of light harvesting capabilities is not considered [*Galbraith et al.*, 2010]. However, how iron limitation of light harvesting capabilities influences the response of oceanic CO_2 uptake to changes in dust deposition has yet to be answered.

2. Methods

The model we use is a coupled global ocean-biogeochemistry model with a detailed iron cycle [*Galbraith et al.*, 2010]. In brief, the biogeochemical model consists of four prognostic tracers, namely phosphate (PO_4), dissolved organic phosphorus (DOP), dissolved iron (Fe) and oxygen (O2). Phytoplankton biomass is modeled as a prognostic variable that is not transported. Export production, grazing and community structure formulations are based on empirical formulations by *Dunne et al.* [2005]. External sources of iron to the ocean are dust deposition and sediment release. The complexation of iron with organic ligands is implicitly calculated as in *Parekh et al.* [2006]. A complete description of the biogeochemical model based on the model code made available by *Galbraith et al.* [2010] is included in the supplemental.

The difference of our approach in comparison to prior approaches is illustrated in the photosynthesis-irradiance (P-I) curve in Figure 1. If increased iron concentrations only increase the maximum photosynthesis, the effect is most pronounced at high light levels. If the impact of iron on light harvesting capabilities is considered as well, also the slope of the response of photosynthesis to irradiance increases. This has a particularly strong effect at low light levels.

The physical ocean model configuration used in this study is described by *Galbraith et al.* [2010, 2011]. The model is the coupled ocean-sea ice model component of the climate

model version 2 with the Modular Ocean Model version 4p1 at coarse resolution (CM2Mc). It has a nominal resolution of 3 degrees in longitudinal direction and 3 degrees in latitudinal direction with a higher resolution up to 2/3 degrees near the equator and at the latitudes of the Drake Passage and the equivalent latitudes on the Northern Hemisphere. The vertical resolution of the model consists of 28 levels with pressure as the vertical coordinate and a free sea surface. The vertical resolution varies from 10 m at the surface to 506 m in the lowest layer. The ocean surface is forced using a repeated climatological year from the Coordinated Ocean Reference Experiment (CORE) [*Griffies et al.*, 2009]. Surface salinities are restored to observations with a time constant of 10 days over the top layer.

We ran the model in a coupled ice-ocean mode with fixed atmospheric forcing and prescribed atmospheric 278 μatm CO_2 for 2500 years as a spinup run. To simulate aeolian deposition of iron a repeated climatological seasonal cycle of dust deposition [*Ginoux et al.*, 2004] is used. Dust deposition is converted to iron deposition assuming a fraction of iron in dust of 3.5 % in clay fractions and 1.2 % in silt fractions and an iron solubility of 2 % following *Galbraith et al.* [2010]. Burial of organic matter or $CaCO_3$ is not allowed in any of our simulations. After the spinup, we applied a dynamic and homogenous atmospheric CO_2 reservoir with an initial value of 590 Pg C [*Sarmiento and Gruber*, 2002] corresponding to 278 atm. The atmospheric CO_2 reservoir is in exchange with the ocean but does not affect temperature. The experiments were started after 200 additional years of spinup with a free atmospheric CO_2 concentration. During these 200 years the change of average surface phosphate concentrations was -6.1×10^{-4} mmol PO_4 m^{-3} and the at-

mospheric CO_2 concentration decreased from 278 atm to 277.81 and to 277.63 atm during the following 1000 years of the control simulation. The decrease is likely due to the small but continuous accumulation of iron from the sediments [*Galbraith et al.*, 2010].

Before starting our model sensitivity experiments, the model was tuned to reproduce observed responses to the two iron fertilization experiments, SOIREE [*Boyd et al.*, 2000] and IRONEXII [*Coale et al.*, 1996], in the same way as *Aumont and Bopp* [2006]. The experiment SOIREE was conducted in the Southern Ocean while IRONEXII in the equatorial Pacific. To simulate the mesoscale iron fertilization experiments the iron concentration was set to 2 nM in the whole mixed layer every 5 degrees in latitudinal and 9 degrees in longitudinal direction and held constant for 30 days. For SOIREE the ocean was fertilized only south of 40°S starting with February in our model and for IRONEXII between 5°S and between 5°N and 140°E and 120°W starting in May. To calculate ΔpCO_2 the simulation was repeated without iron fertilization and the difference in pCO_2 was calculated from these two simulations. Following *Aumont and Bopp* [2006], the response to fertilization was determined from sites that were within ± 10 m difference in the mixed layer depth and ± 2 °C to the respective fertilized location in SOIREE or IRONEXII. The responses in pCO_2 of these fertilization sites give a range of responses that are then compared to the observed values. The model parameters were optimized to reduce the difference between observed and simulated ΔpCO_2. In the resulting parameter set the stability constant of iron-ligand complexes increases from $KFeL_{min} = 8 \times 10^9$ M^{-1}, $KFeL_{max} = 8 \times 10^{10}$ M^{-1} to $KFeL_{min} = 1 \times 10^{11}$ M^{-1}, $KFeL_{max} = 5 \times 10^{11}$ M^{-1}. These values are more in line with a recent compilation by *Gledhill and Buck* [2012] of $KFeL$ being in the range of 10^{11}

to 10^{12} M^{-1}. The half-saturation constant of iron to phosphate uptake ($k_{Fe:P}$) is reduced from 0.8 mmol Fe (mol PO_4)$^{-1}$ to 0.4 mmol Fe (mol PO_4)$^{-1}$ and the mortality rate (λ_0) is increased from 0.19 d^{-1} to 0.38 d^{-1} to better reproduce the observations.

We perform 4 sensitivity experiments to test the importance of iron-light colimitation at different iron concentrations: (i) Abrupt increase of dust deposition to a deposition as estimated for the last glacial maximum [*Mahowald et al.*, 2006] hereafter abbreviated as LGM-ILL. (ii) Equal to (i) but without the impact of iron on light harvesting capabilities (LGM-NOILL). (iii) Abrupt decrease of dust deposition to a deposition as estimated for a climate with double CO_2 concentrations relative to today [*Mahowald et al.*, 2006] hereafter abbreviated as 2xCO_2-ILL. (iv) As (iii) but without the impact of iron on light harvesting capabilities (2xCO_2-NOILL). In addition to the sensitivity experiments the spinup run is continued with a prognostic atmospheric CO_2 reservoir as a control simulation to compare the experiments to (CTL). All dust deposition fields are shown in the Supplementary Figure S1.

The dust deposition used in the control run and the preindustrial estimate by *Mahowald et al.* [2006] differ. To make the experiments independent of the control dust deposition, the dust deposition estimates in the experiments are created by multiplying the dust deposition in the control run with the ratio of the LGM or 2xCO2 dust deposition estimates by *Mahowald et al.* [2006] to the preindustrial estimate by *Mahowald et al.* [2006]. Additional experiments were performed without scaling the change in dust deposition to the preindustrial estimate, thus using the absolute dust deposition fields as simulated by *Mahowald et al.* [2006] (Supplementary Figure S2). In these additional runs more CO_2 is

taken up using the LGM dust and less using the 2xCO2 dust. The impact of iron limitation of light harvesting capabilities, however, is as strong as in the simulations shown here.

Note that we are not trying to realistically simulate past conditions of the last glacial maximum or predictions into the future. Atmospheric forcing, temperature and circulation remain at preindustrial conditions in all our sensitivity experiments and we concentrate our analysis of a more mechanistic parameterization of iron limitation on the isolated impact of changes in aeolian iron supply. Also fraction and solubility of iron in dust in all experiments are kept as in the spinup run for reasons of comparability.

To turn off the effect of iron on light harvesting capabilities in experiments 2) and 4), the variables describing the light harvesting capabilities, the initial slope in the P-I curve (α^{chl}) and the chlorophyll-to-carbon ratio (θ^{Fe}_{max}) (also see the model description in the supplemental), are kept at the annual mean values they have at the end of the spinup run at each point in space. There is thus no seasonal cycle of these variables in the experiments with no iron limitation of light harvesting capabilities whereas in the control experiment α^{chl} and θ^{Fe}_{max} vary seasonally. In a comparison between the control experiment to an additional control experiment (not shown here) in which we fixed α^{chl} and θ^{Fe}_{max} to the annual mean of the last year of the spinup, the differences are very small and, in terms of the atmospheric carbon reservoir, amount to 0.6 atm.

3. Results and Discussion

3.1. Tuning the model

In order to validate the response of the model to changes in iron concentrations, we tune the model to be able to reproduce observed responses to mesoscale iron fertilization experiments in the same way as *Aumont and Bopp* [2006] (Figure 2a). With the original parameter set of *Galbraith et al.* [2010] pCO_2 is much more reduced than observed in SOIREE while with the tuned parameter set the observed values are perfectly within the simulated range of ΔpCO_2. On the other hand, the difference between new and old parameters is not that pronounced in the fertilization experiment IRONEXII. With the new parameter set ΔpCO_2 is underestimated although at the end of the experiment the observed value lies in between of the simulated ranges of original and new parameter set. The root mean square errors (RMSE) for the simulated phosphate, oxygen and iron concentrations compared to observations from the World Ocean Atlas and *Tagliabue et al.* [2012] are 0.30 mmol PO_4 m^{-3}, 34.79 mmol O_2 m^{-3} and 1.0 nM dFe, respectively, using the original parameter set by *Galbraith et al.* [2010]. With the tuned parameter set the RMSE for phosphate does not change, the RMSE for oxygen concentrations increases slightly to 36.73 mmol O_2 m^{-3} and the RMSE for iron concentrations reduces strongly to 0.89 nM dFe for the full ocean and from 0.27 nM dFe to 0.26 nM dFe at the surface. It is encouraging that the model we use is able to reproduce the observed response to iron fertilization during SOIREE in the Southern Ocean and that the agreement to observed iron concentrations is improved with the tuned parameter set.

3.2. Oceanic CO_2 uptake

The LGM dust deposition leads to a total decrease of atmospheric CO_2 by 22.8 atm (Figure 3a) in our model simulations. This decrease is about 19% larger (or 3.7 atm) than that of simulation LGM-NOILL, which does not account for iron-light colimitation. Recent estimates of the CO_2 uptake of the ocean by increasing the dust to LGM conditions have all been smaller than in our idealized model results. The oceanic drawdown of CO_2 in simulations with dust of the last glacial maximum from the literature are 11atm [*Bopp et al.*, 2003], 10 atm [*Parekh et al.*, 2008], 16 atm[*Tagliabue et al.*, 2009b], 25 atm [*Oka et al.*, 2011] and are thus a small part of the full glacial decrease in atmospheric CO_2 of $\sim$50 atm prior to carbonate compensation, i.e. the burial of carbon as $CaCO_3$ in ocean sediments [*Brovkin et al.*, 2007; *Tagliabue et al.*, 2009b]. Particularly the interactive limitation of the phytoplankton in the Southern Ocean by iron and light could produce a strong impact of dust deposition in our experiment LGM-ILL. Our new simulations suggest that dust deposition can have a larger impact on the biological carbon pump than suggested by recent studies, and thus could be a major factor contributing to the reduction of atmospheric CO_2 concentration during glacial times.

The difference of our simulated sensitivity of atmospheric CO_2 already in the NOILL simulations in comparison to other studies stems from differences in the residence time of dissolved iron at the surface. In the model we use, the equilibrium constant between free iron, ligands and their complexation ($KFeL = 1 \times 10^{11}$ to 5×10^{11} M^{-1}) is lower than in other models such as in [*Tagliabue et al.*, 2009b] ($KFeL = 10^{12}$ M^{-1}). In addition, in the model we use, photodissociation of iron-ligand complexes reduces the equilibrium

constant to the lower end of $KFeL = 1 \times 10^{11}$ to 5×10^{11} M^{-1} at the surface. The low equilibrium constant at the surface leads to fast iron scavenging and a short residence time of dissolved iron. The dissolved iron concentrations rely much more on external sources because of the low background concentrations. A further factor reducing the background concentration is the neglect of a hydrothermal source of dissolved iron in our model configuration - although the link of this iron source to biological productivity in the surface ocean has been argued to be negligible [*Tagliabue et al.*, 2014]. The response of the biological pump to changes in iron supply is hence much stronger than with a long residence time of dissolved iron at the surface. For a better estimate of how the oceanic CO_2-uptake changes with a varying degree of iron limitation of phytoplankton, the residence time of iron in surface water needs to be better constrained in observational studies.

For predictions of future atmospheric CO_2 concentrations an estimation of the susceptibility of the ocean biogeochemistry to possible decreases in dust deposition in a warmer and wetter climate is necessary [*Mahowald et al.*, 2006, 2010]. Accounting for the iron limitation of light harvesting capabilities at low dust deposition leads to an extra increase of atmospheric CO_2 by 9.6 atm in experiment 2xCO_2-ILL compared to experiment 2xCO_2-NOILL. This makes up for 32 % of the total response of 28.0 atm and is around twice the CO_2 increase estimated by previous studies. In the modeling study by *Tagliabue et al.* [2014] shutting the dust deposition off completely leads to a slight increase of the atmospheric CO_2 concentration by 2 ppmv. Another modeling study with a different model simulated an increase of 14 atm by reducing current dust deposition by half [*Parekh et al.*, 2006]. Based on observations of interactions between iron and light limitation in

incubation experiments and culture studies [*Greene et al.*, 1991; *Davey and Geider*, 2001; *Hopkinson et al.*, 2007; *Moore et al.*, 2007; *Hopkinson and Barbeau*, 2008] our global model results show that a decrease in dust deposition could lead to a larger decrease in future oceanic CO_2 uptake than estimated previously.

The globally integrated export production shows a strong response to the changes in dust deposition particularly during the first 100 years of the experiments (Figure 3b). The fluctuations on shorter time scales stem from fluctuations in sea ice coverage and are mediated to export production by affecting the irradiance reaching the ocean surface. In the case of the LGM dust, excess macronutrients are taken up and in the case of the 2xCO_2 dust, excess iron is taken up during the first 100 years until in the end global export production equilibrates at a higher (+0.86 Pg C yr^{-1} at 100 dbar) or lower level (-0.94 Pg C yr^{-1} at 100 dbar) relative to the control simulation, respectively. At the end of the simulations the difference in the response of export production between applying and not applying the iron limitation of light harvesting capabilities of phytoplankton is 0.36 Pg C yr^{-1} at 100 dbar in the case of LGM dust and 0.35 Pg C yr^{-1} at 100 dbar in the case of 2xCO_2 dust and thus very pronounced on the globally integrated scale (compare also Supplementary Table S1). The iron limitation of light harvesting capabilities has thus a strong control on the sensitivity of simulated global export production and atmospheric CO_2 concentrations to the supply of iron to the surface ocean.

The regional difference between the experiments with and without consideration of the impact of iron on light harvesting capabilities (LGM-ILL minus LGM-NOILL) reveals that, in comparison to the LGM-NOILL experiment, export production is particularly

increased in the North Pacific, the North Atlantic and the Southern Ocean (Figure 4). Accordingly, surface phosphate concentrations are reduced in these regions. The reason for that is that due to the consideration of iron-light colimitation, growth rates are increased the most at low light (not saturated) levels which leads to the strongest response to iron addition in areas with light limitation (Figure 1). In contrast, in the 2xCO_2-ILL experiment the effect of iron limitation is enhanced so that carbon export is generally reduced, particularly in the northern subtropical Pacific for which a large decline in dust deposition is predicted under global warming (Figure 4). With export production being reduced under 2xCO2, more macronutrients are left unutilized in these regions and can be transported into the more oligotrophic subtropical gyres, where export production can thus increase in the 2xCO2 scenario.

4. Conclusions

Iron-light colimitation is, in contrast to colimitation of, for example, nitrogen and phosphorus, biochemically dependent in that iron is needed for light harvesting antennae and enzymes in the electron transport [*Saito et al.*, 2008]. We show that our model has a higher sensitivity to changes in dust deposition than earlier models and that the direct effect of iron concentrations on light harvesting capabilities of phytoplankton further enhances the model sensitivity to changes in dust deposition. Decreasing dust deposition could decrease oceanic CO_2 uptake, by a larger amount than suggested previously. Furthermore, we show that the CO_2 uptake triggered by LGM dust is up to twice as large in our simulations than estimated before. We suggest that the consideration of the effect of iron on light harvesting has a strong impact on the response of the ocean biogeochemistry to dust deposition.

The influence of iron on light harvesting increases the response of atmospheric CO_2 to dust deposition by 19 % of the total response for the LGM dust deposition and 32 % for the 2xCO_2 dust deposition. Due to the importance of this mechanism, more observational and experimental constraints on iron limitation and colimitation with other nutrients and factors are needed for accurate reconstructions of the past climate and prediction of the future. Small details of nutrient limitation of phytoplankton could have large effects of the oceanic response to changes in dust deposition.

Acknowledgments. We acknowledge financial support from the Deutsche Forschungsgemeinschaft (SFB 754) and thank two anonymous reviewers for their constructive comments and suggestions for improvement. We thank Natalie Mahowald (Cornell University, Ithaca, USA) for sharing the dust deposition estimates, Eric Galbraith (McGill University, Montreal, Canada) and Heiner Dietze (GEOMAR, Kiel, Germany) for helpful discussions, advice and technical support. The model data used to generate the figures will be available at http://thredds.geomar.de/thredds/catalog_open_access.html.

References

Aumont, O., and L. Bopp (2006), Globalizing results from ocean in situ iron fertilization studies, *Global Biogeochemical Cycles*, *20*(2), 1–15, doi:10.1029/2005GB002591.

Behrenfeld, M., and A. Milligan (2013), Photophysiological expressions of iron stress in phytoplankton, *Annual Review of Marine Science*, *5*(January), 217–246, doi: 10.1146/annurev-marine-121211-172356.

Behrenfeld, M., O. Prasil, M. Babin, and F. Bruyant (2004), In search of a physiological basis for covariations in lightlimited and lightsaturated photosynthesis, *Journal of Phycology*, *40*(1), 4–25, doi:10.1046/j.1529-8817.2004.03083.x.

Bopp, L., K. Kohfeld, C. Le Quéré, and O. Aumont (2003), Dust impact on marine biota and atmospheric CO2 during glacial periods, *Paleoceanography*, *18*(2), doi:10.1029/2002PA000810.

Boyd, P. W., and M. J. Ellwood (2010), The biogeochemical cycle of iron in the ocean, *Nature Geoscience*, *3*(10), 675–682, doi:10.1038/ngeo964.

Boyd, P. W., a. J. Watson, C. S. Law, E. R. Abraham, T. Trull, R. Murdoch, D. C. Bakker, a. R. Bowie, K. O. Buesseler, H. Chang, M. Charette, P. Croot, K. Downing, R. Frew, M. Gall, M. Hadfield, J. Hall, M. Harvey, G. Jameson, J. LaRoche, M. Liddicoat, R. Ling, M. T. Maldonado, R. M. McKay, S. Nodder, S. Pickmere, R. Pridmore, S. Rintoul, K. Safi, P. Sutton, R. Strzepek, K. Tanneberger, S. Turner, A. Waite, and J. Zeldis (2000), A mesoscale phytoplankton bloom in the polar Southern Ocean stimulated by iron fertilization., *Nature*, *407*(6805), 695–702, doi:10.1038/35037500.

Brovkin, V., A. Ganopolski, D. Archer, and S. Rahmstorf (2007), Lowering of glacial atmospheric CO2 in response to changes in oceanic circulation and marine biogeochemistry, *Paleoceanography*, *22*(4), 1–14, doi:10.1029/2006PA001380.

Coale, K. H., K. S. Johnson, S. E. Fitzwater, R. M. Gordon, S. Tanner, F. P. Chavez, L. Ferioli, C. Sakamoto, P. Rogers, F. Millero, P. Steinberg, P. Nightingale, D. Cooper, W. P. Cochlan, M. R. Landry, J. Constantinou, G. Rollwagen, a. Trasvina, and R. Kudela (1996), A massive phytoplankton bloom induced by an ecosystem-scale iron fertiliza-

tion experiment in the equatorial Pacific Ocean.

Davey, M., and R. J. Geider (2001), Impact of iron limitation on the Photosynthetic Apparatus of the Diatom Chaetoceros Muelleri (Bacillariophyceae), *Journal of Phycology*, *37*(6), 987–1000, doi:10.1046/j.1529-8817.2001.99169.x.

Dunne, J. P., R. A. Armstrong, A. Gnanadesikan, and J. L. Sarmiento (2005), Empirical and mechanistic models for the particle export ratio, *Global Biogeochemical Cycles*, *19*(4), 1–16, doi:10.1029/2004GB002390.

Feng, Y., C. Hare, J. Rose, S. Handy, G. DiTullio, P. Lee, W. Smith, J. Peloquin, S. Tozzi, J. Sun, Y. Zhang, R. Dunbar, M. Long, B. Sohst, M. Lohan, and D. Hutchins (2010), Interactive effects of iron, irradiance and CO2 on Ross Sea phytoplankton, *Deep Sea Research Part I: Oceanographic Research Papers*, *57*(3), 368–383, doi:10.1016/j.dsr.2009.10.013.

Galbraith, E. D., A. Gnanadesikan, J. P. Dunne, and M. R. Hiscock (2010), Regional impacts of iron-light colimitation in a global biogeochemical model, *Biogeosciences*, *7*, 1043–1064.

Galbraith, E. D., E. Y. Kwon, A. Gnanadesikan, K. B. Rodgers, S. M. Griffies, D. Bianchi, J. L. Sarmiento, J. P. Dunne, J. Simeon, R. D. Slater, A. T. Wittenberg, and I. M. Held (2011), Climate Variability and Radiocarbon in the CM2Mc Earth System Model, *Journal of Climate*, *24*(16), 4230–4254, doi:10.1175/2011JCLI3919.1.

Ginoux, P., J. Prospero, O. Torres, and M. Chin (2004), Long-term simulation of global dust distribution with the GOCART model: correlation with North Atlantic Oscillation, *Environmental Modelling & Software*, *19*(2), 113–128, doi:10.1016/S1364-

8152(03)00114-2.

Gledhill, M., and K. Buck (2012), The organic complexation of iron in the marine environment: a review, *Frontiers in Microbiology*, *3*(February), 1–17, doi: 10.3389/fmicb.2012.00069.

Greene, R. M., R. J. Geider, and P. G. Falkowski (1991), Effect of iron limitation on photosynthesis in a marine diatom, *Limnology and Oceanography*, *36*(8), 1772–1782, doi:10.4319/lo.1991.36.8.1772.

Griffies, S. M., A. Biastoch, C. Böning, F. Bryan, G. Danabasoglu, E. P. Chassignet, M. H. England, R. Gerdes, H. Haak, R. W. Hallberg, W. Hazeleger, J. Jungclaus, W. G. Large, G. Madec, A. Pirani, B. L. Samuels, M. Scheinert, A. S. Gupta, C. A. Severijns, H. L. Simmons, A. M. Treguier, M. Winton, S. Yeager, and J. Yin (2009), Coordinated Ocean-ice Reference Experiments (COREs), *Ocean Modelling*, *26*(1-2), 1–46, doi:10.1016/j.ocemod.2008.08.007.

Hopkinson, B., and K. A. Barbeau (2008), Interactive influences of iron and light limitation on phytoplankton at subsurface chlorophyll maxima in the eastern North Pacific, *Limnology and Oceanography*, *53*(4), 1303–1318.

Hopkinson, B., B. Mitchell, R. Reynolds, H. Wang, K. Selph, C. I. Measures, C. Hewes, O. Holm-Hansen, and K. Barbeau (2007), Iron limitation across chlorophyll gradients in the southern Drake Passage: Phytoplankton responses to iron addition and photosynthetic indicators of iron stress, *Limnology and Oceanography*, *52*(6), 2540–2554.

Mahowald, N. M., D. R. Muhs, S. Levis, P. J. Rasch, M. Yoshioka, C. S. Zender, and C. Luo (2006), Change in atmospheric mineral aerosols in response to climate: Last

glacial period, preindustrial, modern, and doubled carbon dioxide climates, *Journal of Geophysical Research*, *111*(D10), doi:10.1029/2005JD006653.

Mahowald, N. M., S. Kloster, S. Engelstaedter, J. K. Moore, S. Mukhopadhyay, J. R. McConnell, S. Albani, S. C. Doney, A. Bhattacharya, M. A. J. Curran, M. G. Flanner, F. M. Hoffman, D. M. Lawrence, K. Lindsay, P. A. Mayewski, J. Neff, D. Rothenberg, E. Thomas, P. E. Thornton, and C. S. Zender (2010), Observed 20th century desert dust variability: impact on climate and biogeochemistry, *Atmospheric Chemistry and Physics*, *10*(22), 10,875–10,893, doi:10.5194/acp-10-10875-2010.

Martin, J. H. (1990), Glacial-Interglacial CO2 change: the iron hypothesis, *Paleoceanography*, *5*(1), 1–13.

Martínez-Garcia, A., A. Rosell-Melé, S. L. Jaccard, W. Geibert, D. M. Sigman, and G. H. Haug (2011), Southern Ocean dustclimate coupling over the past four million years, *Nature*, pp. 1–5, doi:10.1038/nature10310.

Moore, C., S. Seeyave, A. Hickman, J. Allen, M. Lucas, H. Planquette, R. Pollard, and A. Poulton (2007), Ironlight interactions during the CROZet natural iron bloom and EXport experiment (CROZEX) I: Phytoplankton growth and photophysiology, *Deep Sea Research Part II: Topical Studies in Oceanography*, *54*(18-20), 2045–2065, doi:10.1016/j.dsr2.2007.06.011.

Moore, J. K., and O. Braucher (2008), Sedimentary and mineral dust sources of dissolved iron to the world ocean, *Biogeosciences*, *5*(3), 631–656, doi:10.5194/bg-5-631-2008.

Oka, A., A. Abe-Ouchi, M. O. Chikamoto, and T. Ide (2011), Mechanisms controlling export production at the LGM: Effects of changes in oceanic physical fields

and atmospheric dust deposition, *Global Biogeochemical Cycles*, *25*(2), 1–12, doi: 10.1029/2009GB003628.

Parekh, P., S. Dutkiewicz, M. J. Follows, and T. Ito (2006), Atmospheric carbon dioxide in a less dusty world, *Geophysical Research Letters*, *33*(3), 2–5, doi: 10.1029/2005GL025098.

Parekh, P., F. Joos, and S. A. Müller (2008), A modeling assessment of the interplay between aeolian iron fluxes and iron-binding ligands in controlling carbon dioxide fluctuations during Antarctic warm events, *Paleoceanography*, *23*(4), 1–14, doi: 10.1029/2007PA001531.

Saito, M., T. Goepfert, and J. Ritt (2008), Some thoughts on the concept of colimitation: Three definitions and the importance of bioavailability, *Limnology and Oceanography*, *53*(1), 276–290.

Sarmiento, J., and N. Gruber (2002), Sinks for anthropgenic carbon, *Physics Today*, *55*, 30–36.

Strzepek, R. F., M. T. Maldonado, K. A. Hunter, R. D. Frew, P. J. Harrison, and P. W. Boyd (2011), Adaptive strategies by Southern Ocean phytoplankton to lessen iron limitation: Uptake of organically complexed iron and reduced cellular iron requirements, *Limnology and Oceanography*, *56*(6), 1983–2002, doi:10.4319/lo.2011.56.6.1983.

Strzepek, R. F., K. A. Hunter, R. D. Frew, P. J. Harrison, and P. W. Boyd (2012), Iron-light interactions differ in Southern Ocean phytoplankton, *Limnology and Oceanography*, *57*(4), 1182–1200, doi:10.4319/lo.2012.57.4.1182.

Sunda, W. G., and S. A. Huntsman (1997), Interrelated influence of iron, light and cell size on marine phytoplankton growth, *Nature*, *2051*(1977), 1193–1197.

Tagliabue, A., L. Bopp, and O. Aumont (2008), Ocean biogeochemistry exhibits contrasting responses to a large scale reduction in dust deposition, *Biogeosciences*, *5*(C), 11–24.

Tagliabue, A., L. Bopp, and O. Aumont (2009a), Evaluating the importance of atmospheric and sedimentary iron sources to Southern Ocean biogeochemistry, *Geophysical Research Letters*, *36*(June), 1–5, doi:10.1029/2009GL038914.

Tagliabue, A., L. Bopp, D. Roche, N. Bouttes, J.-C. Dutay, R. Alkama, M. Kageyama, E. Michel, and D. Paillard (2009b), Quantifying the roles of ocean circulation and biogeochemistry in governing ocean carbon-13 and atmospheric carbon dioxide at the last glacial maximum, *Climate of the Past*, *5*, 695–706.

Tagliabue, A., T. Mtshali, O. Aumont, A. R. Bowie, M. B. Klunder, A. N. Roychoudhury, and S. Swart (2012), A global compilation of dissolved iron measurements: focus on distributions and processes in the Southern Ocean, *Biogeosciences*, *9*(6), 2333–2349, doi:10.5194/bg-9-2333-2012.

Tagliabue, A., O. Aumont, and L. Bopp (2014), The impact of different external sources of iron on the global carbon cycle, *Geophysical Research Letters*, *41*, 920–926, doi: 10.1002/2013GL059059.

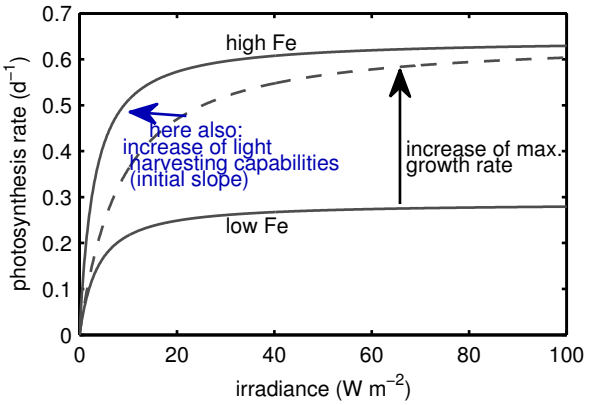

Figure 1. Impact of iron on the photosynthesis irradiance (P-I) curve. The lower solid line represents the P-I curve for low iron concentrations, the upper solid line represents the P-I curve for high iron concentrations in the model we use here. The dashed line represents the P-I curve if a higher iron availability only increases the maximum growth rate and not the light harvesting capabilities.

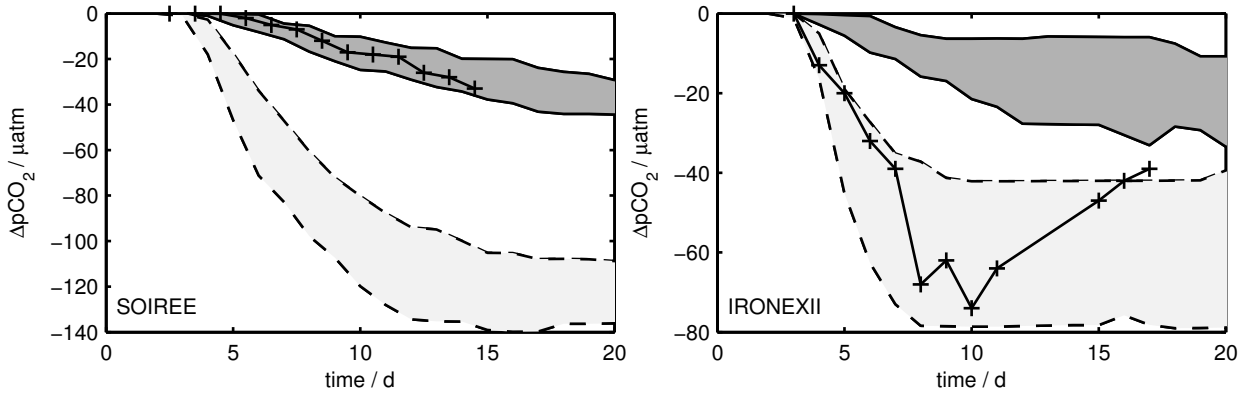

Figure 2. Comparison between observed and simulated response in pCO_2 to mesoscale iron fertilization as in the experiments SOIREE [*Boyd et al.*, 2000] (left) and IRONEXII [*Coale et al.*, 1996] (right). The crosses are observed differences between pCO_2 inside and outside the fertilization area as read by eye from [*Aumont and Bopp*, 2006]. The light shaded area indicates the simulated response with parameters as in *Galbraith et al.* [2010] and the dark shaded area with the new parameter values. Note the different scales.

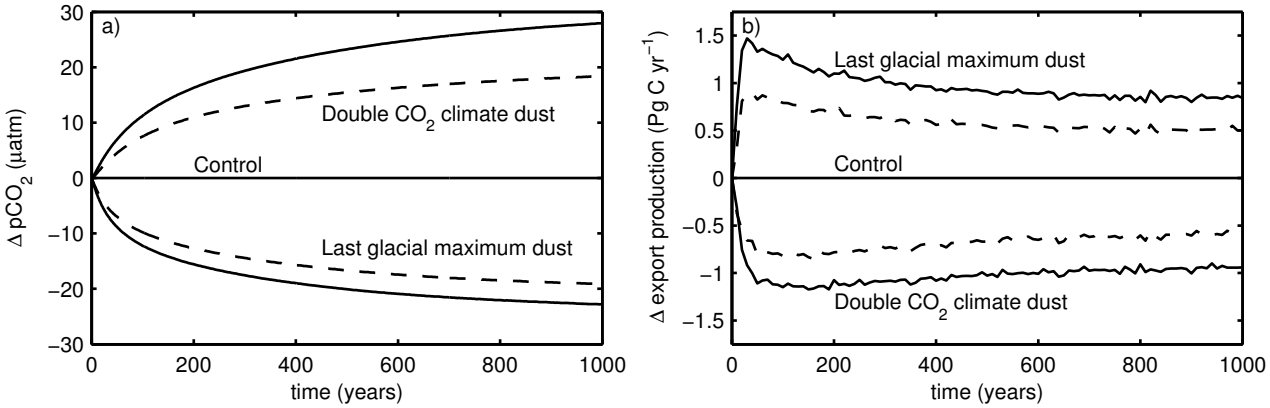

Figure 3. Change of a) atmospheric CO_2 concentration for the $2xCO_2$ dust deposition (upper lines) and for the LGM dust deposition (lower lines) and b) globally integrated export production (at 100 dbar) relative to the control simulation for the LGM dust deposition (upper lines) and for the $2xCO_2$ dust deposition (lower lines). Dashed lines are runs without the dependence of light harvesting capabilites on iron, solid lines are runs with considering the effect of iron on light harvesting capabilities.

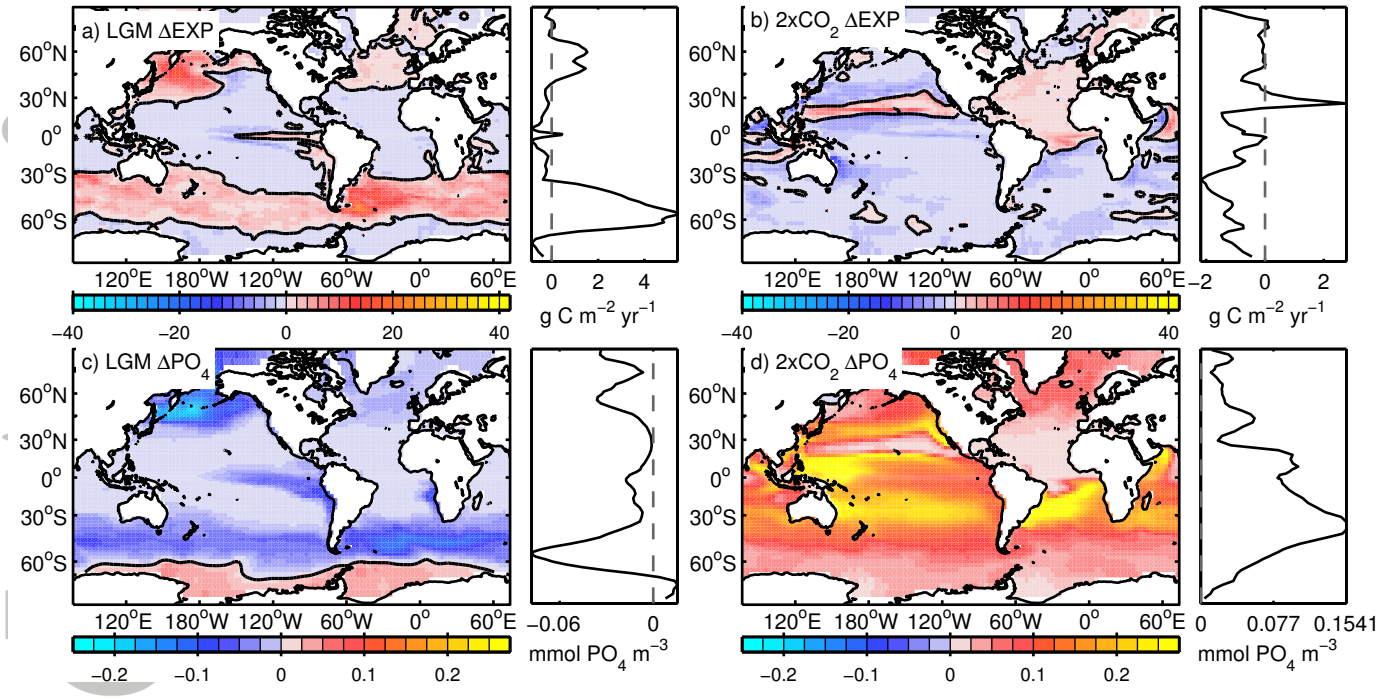

Figure 4. Difference between the simulations with and without considering the effect of iron on light harvesting in export production at 100 dbar (g C m^{-2} yr^{-1}) (first row) and in surface phosphate concentrations (mmol m^{-3}) (second row). The left column shows the results using the LGM dust and the right column the results using the $2xCO_2$ dust. The zonal mean is displayed right to each map.